NMR Evidence for a Short, Strong Hydrogen Bond at the Active Site of a Cholinesterase[†]

Carol Viragh,[‡] Thomas K. Harris,[§] Putta Mallikarjuna Reddy,[‡] Michael A. Massiah,[§] Albert S. Mildvan,*[,§] and Ildiko M. Kovach*[,‡]

Department of Chemistry, The Catholic University of America, Washington, D.C. 20064, Department of Biological Chemistry, Johns Hopkins School of Medicine, Baltimore, Maryland 21205

Received September 26, 2000; Revised Manuscript Received October 26, 2000

ABSTRACT: Cholinesterases (ChE), use a Glu−His−Ser catalytic triad to enhance the nucleophilicity of the catalytic serine. It has been shown that serine proteases, which employ an Asp−His−Ser catalytic triad for optimal catalytic efficiency, decrease the hydrogen bonding distance between the Asp-His pair to form a short, strong hydrogen bond (SSHB) upon binding mechanism-based inhibitors, which form tetrahedral Ser-adducts, analogous to the tetrahedral intermediates in catalysis, or at low pH when the histidine is protonated [Cassidy, C. S., Lin, J., Frey, P. A. (1997) *Biochemistry 36*, 4576−4584]. Two types of mechanism-based inhibitors were bound to pure equine butyrylcholinesterase (BChE), a 364 kDa homotetramer, and the complexes were studied by ^{1}H NMR at 600 MHz and 25−37 °C. The downfield region of the ^{1}H NMR spectrum of free BChE at pH 7.5 showed a broad, weak, deshielded resonance with a chemical shift, $\delta = 16.1$ ppm, ascribed to a small amount of the histidine-protonated form. Upon addition of a 3-fold excess of diethyl 4-nitrophenyl phosphate (paraoxon) and subsequent dealkylation, the broad 16.1 ppm resonance increased in intensity 4.7-fold, and yielded a *D*/*H* fractionation factor $\phi = 0.72 \pm 0.10$ consistent with a SSHB between Glu and His of the catalytic triad. From an empirical correlation of δ with hydrogen-bond length in small crystalline compounds, the length of this SSBH is 2.64 ± 0.04 Å, in agreement with the length of 2.62 ± 0.02 Å independently obtained from ϕ. The addition of a 3-fold excess of *m*-(*N*,*N*,*N*-trimethylammonio)trifluoroacetophenone to BChE yielded no signal at 16.1 ppm, and a 640 Hz broad, highly deshielded proton resonance with a chemical shift $\delta = 18.1$ ppm and a *D*/*H* fractionation factor $\phi = 0.63 \pm 0.10$, also consistent with a SSHB. The length of this SSHB is calculated to be 2.62 ± 0.04 Å from δ and 2.59 ± 0.03 Å from ϕ. These NMR-derived distances agree with those found in the X-ray structures of the homologous acetylcholinesterase complexed with the same mechanism-based inhibitors, 2.60 ± 0.22 and 2.66 ± 0.28 Å. However, the order of magnitude greater precision of the NMR-derived distances establish the presence of SSHBs. We suggest that ChEs achieve their remarkable catalytic power in ester hydrolysis, in part, due to the formation of a SSHB between Glu and His of the catalytic triad.

Acetylcholinesterases (AChE)[1] are of interest to enzymologists because of their critical role in neurotransmission and their high catalytic power (*1*−*5*). AChEs hydrolyze their natural substrate, acetylcholine (ACh), at near the diffusional rate limit at low substrate saturation and with a k_{cat} of $\sim 10^4$ s^{-1} under saturating conditions (*1*−*3*, *5*). Comparison of this k_{cat} with the pseudo-first-order rate constant for the spontaneous hydrolysis of ACh at the same temperature and pH reveals a rate acceleration or catalytic power of 10^{13}-fold. Butyrylcholinesterases (BChE) are very similar in structure and catalytic function, but have a less well-defined role in biological processes (*4*, *5*). Yet the catalytic powers of these enzymes are comparable. The catalytic perfection of cholinesterases (ChE) may be related to a number of factors, one of which is the efficient use of the catalytic triad, the hallmark of serine hydrolase function. The catalytic triad is Ser-200, His-440, and Glu-327 in *Torpedo californica (Tc)* AChE, the first ChE for which an X-ray structure was determined (*6*). Scheme 1 illustrates a mechanism for ChEs (serine hydrolases) showing two proton-transfer steps in acylation and two proton-transfer steps in deacylation (*7*). Proton inventory experiments with AChE and aryl esters and anilides have provided evidence for only one proton transfer in the rate-determining step(s) under k_{cat}/K_m, and k_{cat} condi-

[†] This work was supported by United States Army Medical Research and Material Command Contract DAMD17-98-2-8021 (to I.M.K.), and by National Institutes of Health Grant DK 28616 (to A.S.M.)

* To whom correspondence should be addressed. (A.S.M.) Phone: (410) 955-2038. Fax: (410) 955-5759. E-mail: mildvan@welchlink.welch.jhu.edu. (I.M.K.) Phone: (202) 319-6550. Fax: (202) 319-5381. E-mail: kovach@cua.edu.

[‡] The Catholic University of America.

[§] Johns Hopkins School of Medicine.

[1] Abbreviations: AChE, acetylcholinesterase (acetyl hydrolase); BChE, butyrylcholinesterase; ChE, cholinesterase; *Ee*, *Electric eel*; *Tc*, *Torpedo californica*; BTC, butyrylthiocholine; Chelex-100, polystyrene-divinylbenzene iminodiacetate sodium form; DFP, diisopropyl fluorophosphate; DTNB, 5,5′-dithiobis(2-nitrobenzoic acid); 2-PAM, 2-(hydroxyiminomethyl)-1-methylpyridinium iodide; TMTFA, *m*-(*N*,*N*,*N*-trimethylammonio)trifluoroacetophenone; paraoxon, diethyl 4-nitrophenyl phosphate; sarin, 2-propyl methylphosphono-fluoridate; soman, 2-(3,3-dimethylbutyl)methylphosphono-fluoridate; SSHB, short, strong hydrogen bond; TSP, 3-(trimethylsilyl)propionate-2,2,3,3,-d_4.

10.1021/bi0022644 CCC: $19.00
Published on Web 12/01/2000

Scheme 1

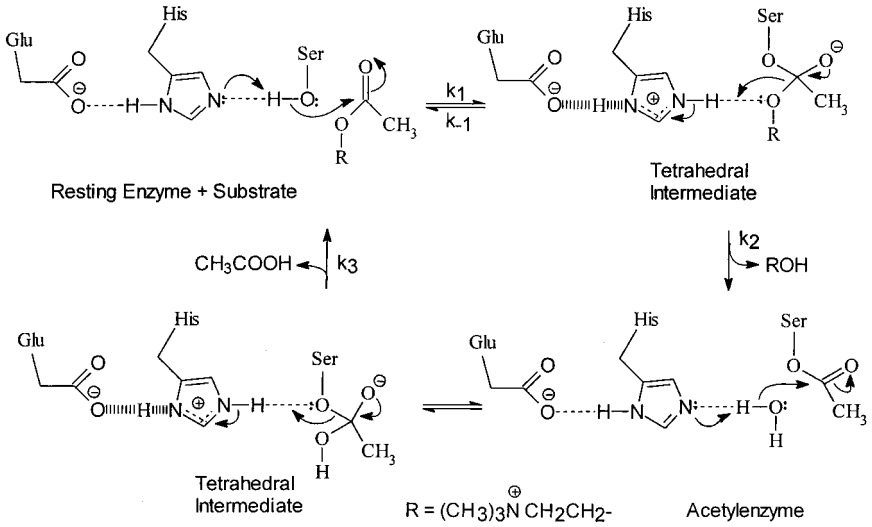

tions in which acylation and deacylation, respectively, are rate limiting (*1*, *8*). Thus, the rate-limiting proton-transfer step occurs either between the catalytic Ser and His or between His and the leaving group, while Glu likely stabilizes the histidinium cation in the transition state.

With serine proteases, several groups have provided evidence for the formation of a short, strong hydrogen bond (SSHB) between Asp and His of the catalytic triad when mechanism-based inhibitors, which form tetrahedral Ser adducts, analogous to the tetrahedral intermediates in catalysis, are bound or at low pH when His becomes protonated (*9*−*13*). While the X-ray structures of serine proteases are consistent with SSHBs between Asp and His of the catalytic triad, 2.5−2.6 **Å** in length, the errors in these hydrogen bond distances (±0.2 to ±0.6 **Å**) are too great to establish this point (*14*−*16*).[2] Higher precision measurements of the lengths of these hydrogen bonds from the *D*/*H* fractionation factors, obtained by NMR, range from 2.49 ± 0.01 to 2.63 ± 0.01 **Å**, supporting the formation of SSHBs (*15*). Similarly, the X-ray structures of *Tc* AChE at low pH (*6*) and in a number of its complexes with mechanism-based inhibitors, which form tetrahedral Ser-adducts, show distances between Glu-327 and His-440 of the catalytic triad ranging from 2.52 ± 0.25 to 2.67 ± 0.23 **Å** (*17*−*19*).[2] While consistent with a SSHB, the large errors in these distances do not rule out a normal hydrogen bond 2.75 **Å** or greater in length, as found in ice (*20*). Molecular dynamics simulations suggested the shortening of the Glu−His distance upon binding of mechanism-based inhibitors to *Tc* AChE (*21*−*23*). These observations, together with the 10^3-fold greater catalytic power of ChEs compared to serine proteases prompted us to use ^{1}H NMR spectroscopy to search for a SSHB in ChEs. NMR criteria for the detection of SSHBs have been set forth (*14*) and have been applied to isomerases, and serine proteases (reviewed in ref *15*). Briefly, the proton in a SSHB is highly deshielded, resulting in a low field ^{1}H resonance between 15 and 19 ppm. The *D*/*H* fractionation factors of such protons are significantly lower than 1.0. Their solvent exchange rates are slowed by at least an order of magnitude, and their strengths, are ≥5 kcal/mol (*14*, *15*).

[2] The errors in interatomic distances determined by protein X-ray crystallography are generally 0.1−0.3 times the atomic resolution (*14*−*16*).

In this paper, we provide evidence for the formation of a SSHB in complexes of equine BChE with two mechanism-based inhibitors, diethyl 4-nitrophenyl phosphate (paraoxon) and *m*-(*N*,*N*,*N*-trimethylammonio)trifluoroacetophenone (TMTFA). Equine BChE is a tetrameric enzyme with a molecular mass of 364 kDa (*24*), which is 6-fold larger than enzymes previously studied by this NMR approach (reviewed in ref *15*). A preliminary abstract of this work has been published (*25*).

EXPERIMENTAL PROCEDURES

Materials. Equine BChE (EC 3.1.1.8) was purchased from Sigma (C1057) and was purified on procainamide Sepharose affinity gel as described (*26*) up to at least 95% purity according to SDS−PAGE. The purity of the enzyme solution was also determined by using the absorbance at 280 nm ($a_{1mg/mL}$ = 1.92) and the Ellman assay (*27*). DTNB and BTC were also from Sigma. Sodium phosphate dibasic was from Fisher Scientific Co. and sodium phosphate monobasic was from Baker. Anhydrous methanol, tetrahydrofuran, diethyl ether, 3-bromoaniline, dimethyl sulfate, *tert*-butyllithium, ethyl trifluoroacetate, iodomethane, potassium carbonate, deuterium oxide (99.96 atom % D), methyl-d_3 alcohol (CD_3-OH), and methyl-d_3 alcohol-*d* (CD_3OD) were purchased from Aldrich Chemical Co. Chelex-100 was from Bio-Rad. TMTFA was prepared as described in the literature (*28*). The intermediate, *m*-(*N*,*N*-dimethylamino)trifluoroacetophenone was purified by successive silica gel column chromatographies. The TMTFA product was further purified by repeated washing with dry ether and dried in vacuo at room temperature. Characterization by NMR confirmed the correct structure (*28*). All solvents and reagents were of analytical or reagent grade and were used without further purification unless otherwise indicated. All buffer solutions used in the NMR experiments were treated with Chelex-100 resin to remove trace paramagnetic metals and filtered through a 0.22 μm filter (Millipore) to remove Chelex particles before addition to NMR samples.

Methods. Inhibition of BChE by TMTFA. The pseudo-first-order rate constant (*k*) for the time-dependent inhibition of BChE by TMTFA was determined by fitting the residual enzyme activity to eq 1:

$$A = (A_0 - A_{inf})e^{-kt} + A_{inf} \quad (1)$$

where A, A_0, and A_{inf} are BChE activities at times t, 0, and infinity respectively, as percents of the activity in absence of TMTFA. Reactions were run at 25.0 ± 0.1 °C in 45 mM sodium phosphate buffer, pH 7.5, containing 25.7 nM BChE and 950 nM TMTFA. Aliquots were drawn at specific time intervals and the residual BChE activity was measured by determining the initial rates (10 s) of hydrolysis of BTC in the presence of DTNB according to Ellman et al. (*27*). The time course of inhibition of equine BChE in the presence of 37-fold excess TMTFA was analyzed by nonlinear least-squares fitting to eq 1 to obtain the pseudo-first-order rate constant for inhibition from which the second-order rate constant (k_{on}) was calculated. Dissociation of EI, as described in eq 2 (in the presence of BTC and DTNB under assay

$$E + I \underset{k_{off}}{\overset{k_{on}}{\rightleftharpoons}} EI \quad (2)$$

conditions), occurred within several minutes.

The initial and the residual enzymatic activities after equilibrium had been reached were used to calculate the apparent dissociation constant, K^{app}, of the enzyme−TMTFA complex. From K^{app} and k_{on}, k_{off} was calculated.

Inhibition of BChE by Paraoxon. The inhibition of equine BChE by paraoxon was rapid at 25 ± 0.1 °C in 45 mM phosphate buffer at pH 7.5 and gave a rate constant of (8.3 ± 0.7) × 10^4 M^{-1} s^{-1}. The time dependence of dealkylation, i.e., the subsequent loss of one ethyl group, under the conditions of the NMR experiment was evaluated by reactivation of the enzyme from the diethyl ester form using 2-PAM as described (*29*).

General NMR Methods. Unless otherwise stated, solution conditions for NMR studies were 0.6 mL of 0.3 mM BChE subunits in 50 mM sodium phosphate buffer (pH 7.5) with 7% (v/v) CD_3OH or 10% (v/v) D_2O. The addition of the ligands, TMTFA and paraoxon, were done at a 3-fold molar excess over the enzyme subunit concentration.

The NMR data were collected on a Varian UnityPlus 600 MHz spectrometer using a Varian 5 mm triple resonance probe. Data were processed on a Silicon Graphics Indigo 2 XZ workstation using the Felix 2.3 software package (Molecular Simulations Inc.). Using the 1331 pulse sequence (*30*) to avoid water excitation, one-dimensional ^{1}H NMR data sets were collected as described (*14*) with the following modifications. The delays between the pulses were adjusted to a maximum excitation at 16.7 ppm (i.e., 12 ppm away from the carrier which is positioned at H_2O) and the acquisition parameters included a 2.5 s relaxation delay, a 512 ms acquisition time, and a 90° pulse width of 30 μs. Chemical shifts are reported with respect to external TSP, and corrected for the temperature.

One-dimensional ^{1}H NMR spectra were collected for free- and TMTFA-bound BChE at 5 and 25 °C with 300 and 1500 transients, respectively. Most of the resonances were very broad at 5 °C, and no NMR signals were detectable downfield of 9 ppm as would be expected for a homotetrameric protein of 364 kDa (*24*). Subsequent spectra of the TMTFA−BChE complex were therefore collected at 25 °C (17 460 transients) and at 34 °C (21 044 transients). With a separate sample, the spectrum of the free enzyme was collected at 25 °C (26 352 transients) as was that of the paraoxon-BChE complex (26 400 transients). The paraoxon−BChE sample was then allowed to dealkylate for 9 days at 22 °C and a spectrum was collected at 25° (76 230 transients). After an additional 10 days of incubation at 4 °C, spectra were again collected at 25 °C, using 1500, 25 700, and 49 000 transients for high *S*/*N*, although the downfield resonance at 16.1 ppm was detectable even after 256 transients. For these latter studies of the paraoxon-BChE adduct, the ^{1}H transmitter offset frequency was moved 1 ppm upfield from water to avoid a pulse-sequence artifact that caused a sharp peak at 16.8 ppm.

To measure the *D*/*H* fractionation factors of the deshielded resonances at maximal sensitivity, the 0.60 mL of TMTFA−BChE sample was divided into two halves. To one-half was added 0.30 mL of an H_2O solution containing 50 mM sodium phosphate buffer, pH 7.5, and 7.0% (v/v) CD_3OH. To the other half was added 0.30 mL of an otherwise identical solution in 99.9% D_2O and 7.0% (v/v) CD_3OD. The NMR spectra of both of the TMTFA−BChE samples were collected at 34 °C, using 57 320 transients each, with the sample in 100% H_2O collected first, permitting the 50% D_2O sample to equilibrate for 3 days. The data on both samples were collected and processed identically. The same general procedure was followed for the paraoxon-BChE samples, but using as diluents, 0.30 mL of 50 mM sodium phosphate buffer pH 7.5 in either 9.99% or 99.9% D_2O (v/v), and the NMR spectra of both samples were collected at 37 °C with 45 400 transients.

The fractionation factor (ϕ), which measures the preference of a hydrogen-bonded site for deuterium over protium, relative to solvent, provides a measure of the hydrogen bond length. As discussed in detail elsewhere (*14*, *15*), a hydrogen-bonded proton vibrates in one of two potential energy wells, each centered at one covalent bond length from the donor and acceptor heavy atoms. As the hydrogen bond becomes shorter, these wells approach each other, becoming broader and shallower. The latter effect decreases the zero point vibrational energy of the hydrogen-bonded proton. Because of the 2-fold greater mass of a deuteron, its zero point vibrational energy decreases ~$(2)^{1/2}$-fold less, resulting in a decreased preference for deuterium over protium (ϕ) as the hydrogen bond shortens. Using quartic potential functions, Bao et al. have derived a graph relating ϕ values to distances between the two proton wells (*12*). With this graph, we have determined distances between the two proton wells from measured ϕ values and have shown that precise hydrogen bond lengths can be obtained by adding two covalent bond lengths to this distance (*14*, *15*).

RESULTS AND DISCUSSION

Kinetics of Inhibition of BChE by TMTFA. From the time-dependent inhibition of BChE at excess inhibitor concentrations (Figure 1), k_{on} = (1.4 ± 0.4) × 10^4 M^{-1} s^{-1} is obtained at pH 7.5 and 25.0 ± 0.1 °C. From the initial and equilibrium concentrations of free enzyme, (Figure 1) the apparent dissociation constant (K^{app}) for EI is 91 ± 10 nM. Hence $k_{off} = k_{on}K^{app}$ = (1.3 ± 0.3) × 10^{-3} s^{-1}. The association of TMTFA with BChE is ~10-fold slower than with AChE, while K^{app} is ~1000-fold greater with BChE. Hence, the k_{off} of TMTFA from BChE is ~100-fold greater than from

Table 1: NMR Properties of Hydrogen-Bonded Protons of BChE

adduct	δ^a (ppm)	ϕ	k_{ex} (s^{-1})^b	distance (Å) from δ	distance (Å) from ϕ	distance (Å) from X-ray
none	16.1		<1700	2.64 ± 0.04		2.52 ± 0.25[c]
paraoxon[d]	16.1	0.72 ± 0.10	<1700	2.64 ± 0.04	2.62 ± 0.02	2.60 ± 0.22[e]
TMTFA	18.1	0.63 ± 0.10	<2000	2.62 ± 0.04	2.59 ± 0.03	2.66 ± 0.28[f]

[a] Errors in δ are ± 0.05 ppm. [b] From π (line width) = $1/T_2$ of the resonance. [c] Free AChE, pH 5.8 (*6*, *17*) [d] Dealkylated, yielding the ethyl-phosphoserine-diester. [e] AChE-soman adduct (*19*). [f] AChE-TMTFA adduct (*17*).

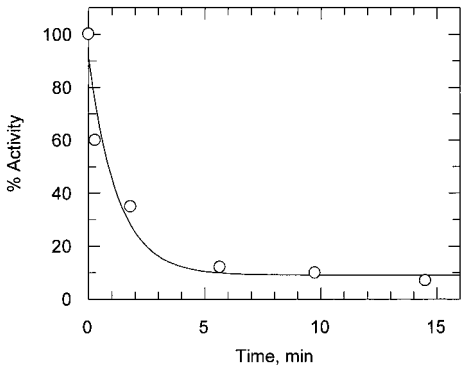

FIGURE 1: Time course of the inhibition of equine BChE by TMTFA. Components present were 45 mM sodium phosphate, pH 7.4, 25.7 nM BChE and 950 nM TMTFA at 25.0 ± 0.1 °C.

AChE. However, to appreciate the intrinsic affinity of TMTFA for ChEs, the equilibrium constant for hydration of TMTFA ($K_{hyd} = 6.2 \times 10^4$) is used for correction (*28*), which then gives the intrinsic dissociation constant, $K = 1.5$ pM.

Interaction of Paraoxon with BChE. The downfield region of the proton NMR spectrum of BChE (0.3 mM subunits) at 25 °C, pH 7.5 showed, after 26 352 transients, only a broad, weak resonance at 16.1 ppm with a *S*/*N* of 3.5 and a width of 550 Hz (Figure 2A). The addition of a 3-fold excess of paraoxon rapidly inactivated the enzyme. Inability to restore activity with 2-PAM indicated that dealkylation had also occurred, leaving an ethyl-phosphoserine-diester on the enzyme, an analogue of the tetrahedral intermediates in catalysis. A 2.9-fold longer NMR accumulation (76 230 transients) revealed an order of magnitude increase in intensity of the signal at 16.1 ppm (*S*/*N* = 28) with no change in its resonance width (546 Hz) (Figure 2B). The 2.9-fold longer accumulation alone would have resulted in only a 1.7-fold increase in *S*/*N*. Hence, the true intensity of the 16.1 ppm resonance increased by 4.7-fold on forming the ethyl-phosphoserine-diester, indicating the approximately stoichiometric formation of a SSHB in the chemically modified enzyme. This hydrogen bond is likely to be at the active site, since the signal intensification occurred in a dealkylated sample in which His-438 is cationic and hydrogen bonded to Glu-325 at the active site and forms a salt-bridge with a phosphate oxygen of the Ser-198 adduct (*2*, *17*, *21*, *22*).

To measure the *D*/*H* fractionation factor of the 16.1 ppm signal, in the ethyl phosphoserine diester, NMR spectra of two samples, one in 45.05% H_2O and the other in 90.01% H_2O were collected and processed under identical conditions, as described in the Experimental Procedures. The relative intensity of the 16.1 ppm resonance in 45.05 and in 90.01% H_2O, measured by integration, was 0.577 ± 0.034, leading to a fractionation factor (ϕ) of 0.72 ± 0.10. This value, significantly lower than 1.0, confirms the formation of a SSHB.

Interaction of TMTFA with BChE. TMTFA forms a tetrahedral Ser-adduct at the active site of AChE, analogous to the tetrahedral intermediates in catalysis, as found by X-ray studies (*17*). The addition of a 3.3-fold excess of TMTFA to 0.3 mM BChE subunits at pH 7.5 and 25 °C yielded a broad, highly deshielded proton resonance at 18.1 ppm and no signal at 16.1 ppm, indicating the formation of a SSHB. Raising the temperature to 34 °C resulted in a 1.2-fold narrowing of the 18.1 ppm signal ($E_{act} = -3.8$ kcal/mol) with significant improvement in *S*/*N*, indicating slow exchange on the NMR time scale (Table 1). Hence, subsequent studies were done at 34 °C where the *S*/*N* was 22 and the resonance width was 640 Hz (Figure 2C). The resonance widths (540−640 Hz) of both the paraoxon and TMTFA adducts are consistent with the homotetrameric molecular weight of 364 kDa for this enzyme (*24*).

To measure the *D*/*H* fractionation factor of the 18.1 ppm signal at maximal sensitivity, NMR spectra of two samples, one in 100% H_2O and the other in 50% H_2O, were collected and processed under identical conditions, as described in Experimental Procedures. The relative intensity of the 18.1 ppm resonance in 50 and 100% H_2O, measured by integration, was 0.615 ± 0.038, leading to a fractionation factor (ϕ) of 0.63 ± 0.10, confirming the formation of a SSHB. The fact that this hydrogen bond forms on binding the mechanism-based inhibitor TMTFA indicates it to be at the active site, very likely between Glu-325 and His-438.

Determination of the Lengths of the SSHB in the BChE Adducts. Chemical shifts and fractionation factors provide precise and independent measurements of hydrogen bond lengths (*14*,*15*). A correlation of hydrogen bond distances (*D*) for 12 crystalline imidazolium-carboxylate complexes from small-molecule high-resolution X-ray diffraction, with proton chemical shifts (δ) obtained by solid-state NMR studies of the same crystals (*31*), is well fitted by the empirical relationship (Figure 3):

$$D = 1.99 + 0.198 \ln(\delta) + (10.14/\delta)^5 \qquad (3)$$

From eq 3, the chemical shift of 18.1 ± 0.05 ppm for the BChE−TMTFA adduct yields a hydrogen bond length of 2.62 ± 0.04 Å (Table 1). Independently, the fractionation factor $\phi = 0.63 \pm 0.10$ yields a distance between the two proton wells of 0.59 ± 0.03 Å. Adding two covalent bond lengths (2.00 Å) to this distance yields a hydrogen bond length of 2.59 ± 0.03 Å. This simple addition assumes the hydrogen bond to be linear. If the hydrogen bond were bent, its length would be even shorter (*14*, *15*). The 2.8 Å X-ray structure of the AChE−TMTFA complex reveals a hydrogen bond between Glu-327 and His-440, 2.66 ± 0.28 Å in length

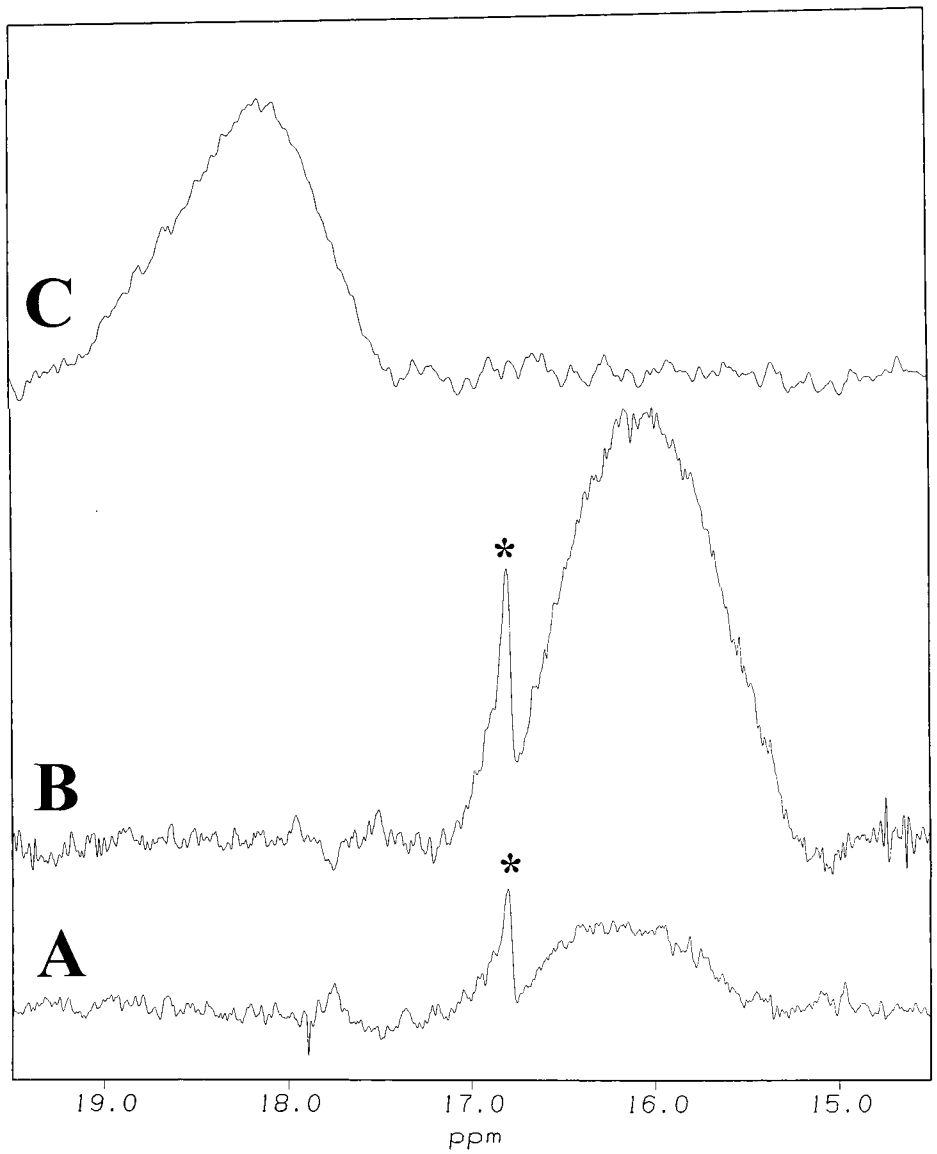

FIGURE 2: Downfield region of the ^{1}H NMR spectrum of BChE and its complexes. (A) Free enzyme (0.3 mM subunits) in 50 mM sodium phosphate buffer, pH 7.5, containing 10% D_2O at 25 °C. Number of scans = 26 352. The narrow signal at 16.8 ppm labeled with an asterisk is an electronic artifact, unrelated to the sample, which is removable by shifting the carrier frequency away from the water resonance. (B) Enzyme (0.3 mM subunits) after treatment with 0.9 mM paraoxon and subsequent dealkylation. Number of scans = 76 230. Components and conditions are otherwise as described in panel A. (C) Enzyme (0.3 mM subunits) treated with 1.0 mM TMTFA in 50 mM sodium phosphate buffer, pH 7.5, containing 7% CD_3OH at 34 °C. Number of scans = 21 044.

Scheme 2

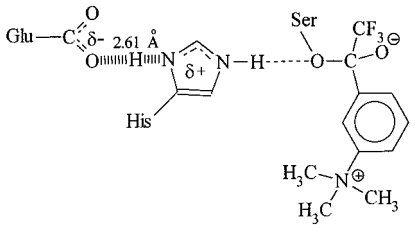

Scheme 3

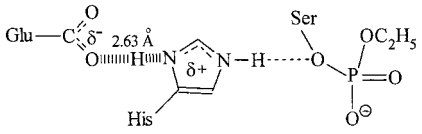

(*17*). Hence, all measurements are in agreement, but the more precise distances obtained by NMR establish the presence of a SSHB in the Glu−His−Ser catalytic triad of this serine hydrolase (Table 1). Scheme 2 illustrates the position and the average length of the SSHB in the BChE−TMTFA complex.

For the dealkylated paraoxon adduct, the chemical shift of 16.1 ppm indicates a slightly longer hydrogen bond. From eq 3, this hydrogen bond length is 2.64 ± 0.04 Å in the presence of the ethyl-phosphoserine-diester (Table 1). From the fractionation factor of this resonance, $\phi = 0.72 \pm 0.10$, a comparable distance of 2.62 ± 0.02 **Å** is calculated (Table 1, Scheme 3). Crystal structures of the soman, sarin, and DFP adducts of AChE, which had undergone dealkylation, show hydrogen-bond lengths between His-440 and Glu-327 which range from 2.53 to 2.67 Å with large errors of ±0.26 to ±0.23 Å, respectively (*19*) (Table 1).

The 4.7-fold weaker signal at 16.1 ppm found in free BChE (Figure 1A) suggests a slight population of the hydrogen-bonded state. On the basis of the upper limit pK_a of 6.6, reported for the acylation of AChE (*1*), His-438 would

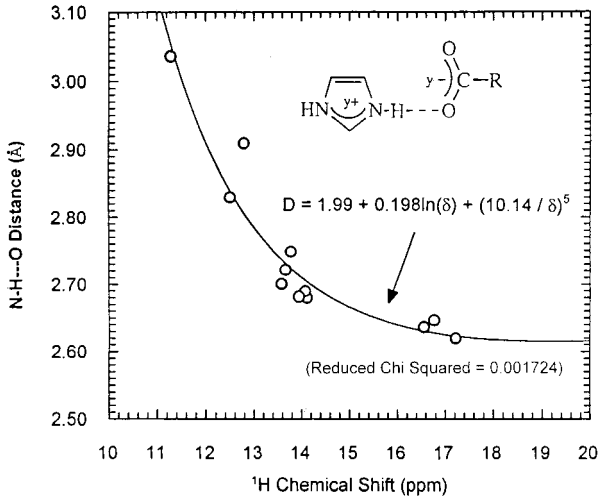

FIGURE 3: Correlation of imidazolium-carboxylate hydrogen bond distances (*D*) from high resolution, small molecule X-ray diffraction with proton chemical shifts (δ) from solid-state NMR studies of crystalline amino acids. The data from ref *31* are fitted by the indicated equation.

be 11% protonated at pH 7.5, which would result in the formation of a SSHB bond analogous to that found in acid chymotrypsin (*12*). The covalent binding and subsequent dealkylation of paraoxon shifts the equilibrium, converting all of the enzyme to the hydrogen-bonded form.

In conclusion, the remarkable catalytic power that ChEs exert in catalyzing the hydrolysis of their natural substrates may result in part from shortening the distance between Glu and His residues of the catalytic triad as His becomes protonated in the rate-determining step. Such formation of a SSHB between Glu and His (Scheme 1) would increase the basicity of His, facilitating the deprotonation of Ser, and the formation of the tetrahedral intermediate. The strength of this SSHB may be estimated to be *at least* 4.9 kcal/mol on the basis of the ≥3150-fold decrease in activity of the Glu-334-Ala mutant of the human AChE (*32*). Hence, the ≥3150-fold contribution of Glu-334 to catalysis could result from its increasing the pK_a of the catalytic His by at least 3.5 units to a value of ≥10, more closely approaching that of the Ser to be deprotonated.

ACKNOWLEDGMENT

The provision of facilities and helpful consultations is gratefully acknowledged to Dr. Ashima Saxena and Dr. Chunyuan Luo of the Division of Biochemistry, WRAIR, Washington, DC.

REFERENCES

1. Quinn, D. M. (1987) *Chem. Rev. 87*, 955−975.
2. Kovach, I. M. (1988) *J. Enzyme Inhib. 2*, 199−208.
3. Quinn, D. M., Pryor, A. N., Selwood, T., Lee, B. H., Acheson, S. A., and Barlow, P. N. (1991) in *Cholinesterases: Structure, Function, Mechanism, Genetics, and Cell Biology* (Massoulie, J., Bacou, F., Barnard, E., Chatonnet, A., Doctor, B. P., and Quinn, D. M., Eds.) pp 252−257, American Chemical Society, Washington, DC.
4. Massoulie, J., Pezzementi, L., Bon, S., Krejci, E., and Valette, F. M. (1993) *Prog. Neurobiol. (Oxf.) 41*, 31−91.
5. Taylor, P., and Radic, Z. (1994) *Annu. Rev. Pharmacol. Toxicol. 34*, 281−320.
6. Sussman, J. L., Harel, M., Frolow, F., Oefner, C., Goldman, A., Toker, L., and Silman, I. (1991) *Science 253*, 872−879.
7. Enyedy, I. J., Kovach, I. M., and Brooks, B. R. (1998) *J. Am. Chem. Soc. 120*, 8043−8050.
8. Kovach, I. M., Larson, M., and Schowen, R. L. (1986) *J. Am. Chem. Soc. 108*, 3054−3056.
9. Robillard, G., and Shulman, R. G. (1974) *J. Mol. Biol. 86*, 541−558.
10. Cassidy, C. S., Lin, J., and Frey, P. A. (1997) *Biochemistry 36*, 4576−4584.
11. Lin, J., Westler, W. M., Cleland, W. W., Markley, J. L., and Frey, P. A. (1998) *Proc. Natl. Acad. Sci. U.S.A. 95*, 14664−14668.
12. Bao, D., Huskey, W. P., Kettner, C. A., and Jordan, F. (1999) *J. Am. Chem. Soc. 121*, 4684−4689.
13. Halkides, C. J., Wu, Y. Q., and Murray, C. J. (1996) *Biochemistry 35*, 15941−15948.
14. Mildvan, A. S., Harris, T. K., and Abeygunawardana, C. (1999) *Methods Enzymol. 308*, 219−245.
15. Harris, T. K., and Mildvan, A. S. (1999) *Proteins: Struct., Funct., Genet. 35*, 275−282.
16. Lipscomb, W. N. (1980) in *Methods for Determining Metal Ion Environments in Proteins* (Darnall, D. W., and Wilkins, R. G., Eds.) pp 265−302, Elsevier, New York.
17. Harel, M., Quinn, D. M., Nair, H. K., Silman, I., and Sussman, J. L. (1996) *J. Am. Chem. Soc. 118*, 2340−2346.
18. Millard, C. B., Koellner, G., Ordentlich, A., Shafferman, A., Silman, I., and Sussman, J. L. (1999) *J. Am. Chem. Soc. 121*, 9883−9884.
19. Millard, C. B., Kryger, G., Ordentlich, A., Greenblatt, H. M., Harel, M., Raves, M. L., Segall, Y., Barak, D., Shafferman, A., Silman, I., and Sussman, J. L. (1999) *Biochemistry 38*, 7032−7039.
20. Brill, V. R., and Tippe, A. (1967) *Acta Crystallogr. 23*, 343−345.
21. Bencsura, A., Enyedy, I., and Kovach, I. M. (1996) *J. Am. Chem. Soc. 118*, 8531−8541.
22. Bencsura, A., Enyedy, I., and Kovach, I. M. (1995) *Biochemistry 34*, 8989−8999.
23. Kovach, I. M. (1998) in *Structure and Function of Cholinesterases and Related Proteins* (Doctor, B. P., Taylor, P., Quinn, D. M., Rotundo, R. L., and Gentry, M. K., Eds.) pp 339−344, Plenum Press, New York and London.
24. Altamirano, C. V., and Lockridge, O. (1999) *Biochemistry 38*, 13414−13422.
25. Viragh, C., Harris, T. K., Reddy, P. M., Massiah, M. A., Mildvan, A. S., and Kovach, I. M. (2001) *Abs. Biophys. Soc.* (in press)
26. De La Hoz, D., Doctor, B. P., Ralston, J. S., Rush, R. S., and Wolfe, A. D. (1986) *Life Sci. 39*, 195−199.
27. Ellman, G. L., Courtney, K. D., Andres, V., and Featherstone, R. M. (1961) *Biochem. Pharmacol. 7*, 88−95.
28. Nair, H. K., Lee, K., and Quinn, D. M. (1993) *J. Am. Chem. Soc. 115*, 9939−9941.
29. Masson, P., Froment, M. T., Bartels, C. F., and Lockridge, O. (1997) *Biochem. J. 325*, 53−61.
30. Turner, D. L. (1983) *J. Magn. Reson. 54*, 146−148.
31. Wei, Y., and McDermott, A. E. (1999) in *Modeling NMR Chemical Shifts: Gaining Insights into Structure and Enviroment* (Facelli, J. C., and de Dios, A. C., Eds.) pp 177−193, Oxford University Press, Cary, NC.
32. Shafferman, A., Kronman, C., Flashner, Y., Leitner, M., Grosfeld, H., Ordentlich, A., Gozes, Y., Cohen, S., Ariel, N., Barak, D., Harel, M., Silman, I., Sussman, J. L., and Velan, B. (1992) *J. Biol. Chem. 267*, 17640−17648.

BI0022644